Rheology and Morphology of Reactively Compatibilized PP/PA6 Blends

Dean Shi, Zhuo Ke, Jinghui Yang, Ying Gao, Jing Wu, and Jinghua Yin*

State Key Laboratory of Polymer Physics and Chemistry, Changchun Institute of Applied Chemistry, Chinese Academy of Sciences, Changchun 130022, P. R. China

Received April 15, 2002

ABSTRACT: This work aims to use the Palierne emulsion type model to describe the relationship between the rheological response to small amplitude oscillatory deformation and morphology of polypropylene/polyamide 6 (PP/PA6) blends compatibilized with maleic anhydride grafted polypropylene (PP-*g*-MAH). It was found that the Palierne emulsion type model could describe very well the linear viscoelastic responses of binary uncompatibilized PP/PA6 blends and failed to describe the ternary compatibilized PP/PP-*g*-MAH/PA6 blends. These features could be attributed to the fact that the morphology of the ternary blends was not of the emulsion type with the PA6 particles dispersed in the PP matrix but of an emulsion-in-emulsion type, i.e., PA6 particles dispersed in the PP matrix themselves contained PP or PP-*g*-MAH inclusions. By consideration of PP-in-PA6 particles as pure PA6 particles, where the volume fraction of the PA6 phase was increased accordingly, the Palierne emulsion type model could work very well for a ternary blending system. Preshear at low frequencies modified the morphology of both binary and ternary blends. The particles of the dispersed phase (PA6) became more uniform. These results suggested that the Palierne emulsion type model could be used to extract information on rheological properties and interfacial tension of polymer blends from known morphology and vice versa.

1. Introduction

It is the common practice to make new materials by blending or alloying different polymers.[1−4] However, most polymers are thermodynamically immiscible and phase-separated upon blending. Compatibilization is thus often necessary for reducing the scale of dispersion, stabilizing the morphology and enhancing interfacial adhesion. This can be achieved by adding a premade block copolymer to the system (nonreactive compatibilization) or by carrying out an in situ reaction between the complementary groups of the blend components (reactive compatibilization).[5]

It is known that the mechanical properties of the composite are strongly related to its morphologies. During the past few decades, a large effect has been made to study the relationship between viscoelastic properties of blending component and the final morphology of polymer blends. Some theoretical models have been developed to study the linear viscoelastic behavior of polymer blends under flow.[6−25] These models relate the dynamic response of polymer blends in their morphology, composition, and interfacial tension between the phases of the blends. Brahimi et al.[21] showed that the complex viscosity of polyethylene/polystyrene blends was very sensitive to the concentration and the structure of the block copolymer. An emulsion model[26] of two viscoelastic liquids with interfacial tension was good enough for uncompatibilized blends and not for blends with an externally added interfacial agent. Graebling et al.[22] studied PDMS/POE-DO blends with and without an externally added interfacial agent and obtained a good agreement between experimental data and theoretical predictions of a simplified version of the Palierne model.[23] This simplified model relates the terminal relaxation process of the blend to the geometrical relaxation of the inclusions. On the basis of this model, they determined the expected reduction of the interfacial tension due to the addition of a relatively small amount of the interfacial agent. Germain et al.[24] investigated the influence of adding a block copolymer on the rheological behavior of PP/PA blends. Using a two-phase Oldroyd model, they concluded that the low shear rate behavior is dominated by the copolymer encapsulating the nodular dispersed phase. Remain et al.[27] showed that upon addition of block copolymers, there is not only the relaxation process mentioned earlier occurring but also an additional relaxation process. Its relaxation time was related, using an expanded version of the Palierne model, to an interfacial shear modulus. Recently, Puyvelde et al. gave an interesting overview on the subject.[28]

How does the Palierne type model describe reactively compatibilized polymer blends? An important effect of the interfacial reaction is the modification of the interfaces from "bare interfaces" to "occupied interfaces". As the extent of the interfacial reaction increases, the interfaces are progressively occupied. O'Shaughnessy et al.[29] concluded that in addition to reducing the interfacial tension, "occupied interfaces" are much less keen to coalescence mainly because of steric hindrance effect. Moreover, there is a "saturated" value of interfacial tension in reactive blending systems. Before the reactions can position sufficient copolymers at the interfaces to substantially diminish interfacial tension, the reaction rates have become exponentially suppressed by steric crowding because of the in situ formed copolymer. Asthana et al.[30] found that an interfacial reaction resulted in reduction in particle size of the dispersed phase and in interfacial tension between the two components of the blend. The interfacial tension decreased with increasing extent of the interfacial reaction. Compared with the nonreactive blends, there was an additional relaxation mechanism occurring in reactive blends leading to enhanced storage modulus.

The aim of this work was to build a way to describe the relationship between the rheological response to small amplitude oscillatory deformation and morphology

* To whom all correspondence should be addressed.

10.1021/ma020595d CCC: $22.00
Published on Web 09/13/2002

for compatibilized blending systems on the basis of Palierne emulsion type model. The blending systems were based on polypropylene (PP) and polyamide 6 (PA6). A maleic anhydride modified PP was used as the reactive interfacial agent. The issue concerning the existence of a "saturated" value for interfacial tension in reactive polymer blends was also discussed.

2. Theoretical Background

The Palierne model can be used to predict the linear viscoelastic behavior of concentrated emulsions of incompressible viscoelastic materials in the presence of an interfacial agent.[22] An expanded version of the model is available and can be shown in the following form[31]

$$G_b^*(\omega) = G_m^*(\omega)\frac{1 + 3\int_0^\infty \frac{E(\omega,R)}{D(\omega,R)}\nu(R)\,dR}{1 - 2\int_0^\infty \frac{E(\omega,R)}{D(\omega,R)}\nu(R)\,dR} \quad (1)$$

where

$$E(\omega,R) = [G_i^*(\omega) - G_m^*(\omega)][19G_i^*(\omega) + 16G_m^*(\omega)] + \frac{4\alpha}{R}[5G_i^*(\omega) + 2G_m^*(\omega)] + \frac{\beta_1^*(\omega)}{R}[23G_i^*(\omega) - 16G_m^*(\omega)] + \frac{2\beta_2^*(\omega)}{R}[13G_i^*(\omega) + 8G_m^*(\omega)] + \frac{24\beta_1^*(\omega)\alpha}{R^2} + 16\beta_2^*(\omega)\frac{\alpha + \beta_1^*(\omega)}{R^2}$$

$$D(\omega,R) = [2G_i^*(\omega) + 3G_m^*(\omega)][19G_i^*(\omega) + 16G_m^*(\omega)] + \frac{40\alpha}{R}[G_i^*(\omega) + G_m^*(\omega)] + \frac{2\beta_1^*(\omega)}{R}[23G_i^*(\omega) + 32G_m^*(\omega)] + \frac{4\beta_2^*(\omega)}{R}[13G_i^*(\omega) + 12G_m^*(\omega)] + \frac{48\beta_1^*(\omega)\alpha}{R^2} + 32\beta_2^*(\omega)\frac{\alpha + \beta_1^*(\omega)}{R^2}$$

$G_b^*(\omega)$ = complex modulus of polymer blend

$G_i^*(\omega)$ = complex modulus of dispersed phase

$G_m^*(\omega)$ = complex modulus of matrix

$\beta_1^*(\omega)$ = surface dilatation modulus

$\beta_2^*(\omega)$ = surface shear modulus

R = dispersed particle radius

$\nu(R)$ = distribution function of dispersed particle radius

α = interfacial tension

ω = deformation frequency

In the linear viscoelastic zone, the deformation of dispersed phase is small and it can be assumed that $\beta_1^*(\omega) = \beta_2^*(\omega) = 0$. Thus, according to the literature,[22] if the interfacial tension between the matrix and the dispersed phase is assumed to be independent of local shear and variation of interfacial area and the particle size distribution of the dispersed phase is narrow enough ($\{R_v\}/\{R_n\} \leq 2$), then eq 1 can be reduced to

$$G_b^*(\omega) = G_m^*(\omega)\frac{1 + 3\sum_i \varphi_i H_i(\omega)}{1 - 2\sum_i \varphi_i H_i(\omega)} \quad (2)$$

where

$$H_i(\omega) = \left(4\left(\frac{\alpha}{R_V}\right)(2G_m^*(\omega) + 5G_i^*(\omega)) + (G_i^*(\omega) - G_m^*(\omega))(16G_m^*(\omega) + 19G_i^*(\omega))\right)\Big/\left(40\left(\frac{\alpha}{R_V}\right)(G_m^*(\omega) + G_i^*(\omega)) + (2G_i^*(\omega) + 3G_m^*(\omega))(16G_m^*(\omega) + 19G_i^*(\omega))\right)$$

R_v = volume average particle radius; $R_v = \frac{\sum_i \varphi_i R_i}{\varphi}$

φ_i = volume fraction of dispersed phase.

If both the continuous and dispersed phases are described by a single Maxwell model, as in the case of the paper of Graebling et al.,[22] eq 2 will yield a distinct plateau at low frequencies. The interfacial tension between the two phases can then be determined by the location and magnitude of this secondary plateau. Its location is dictated by several parameters. For example, it shits toward lower frequency and lower storage modulus with increasing zero shear viscosity ratio, K, between the inclusion, η_i, and the matrix, η_m. Reducing the interfacial tension also shifts it toward lower frequency. Moreover, its width will increase. The secondary plateau becomes less distinct when the particle size distribution is broader. The relaxation time ratio between the inclusion and the matrix χ ($\chi = \lambda_i/\lambda_m$, λ_i and λ_m are relaxation times of the inclusion and matrix, respectively) has also an effect on it. When it approaches 1, it becomes ill-defined. As the volume fraction of the disperse phase increases, the secondary plateau becomes more pronounced in width and shifts toward higher frequencies. Sometimes, when the secondary plateau is ill-defined, simulating experimental data in the whole range of testing frequency could yield useful information such as interfacial tension. This is the main subject of the study reported in this paper.

Besides the Palierne emulsion model, the Oldroyd[7] model and the Choi and Schowalter model[25] are also widely used in polymer blends in the dilute and semidilute regimes to predict their rheological behavior. However, they are not used in this study because they are supposed to describe only the low-frequency region rheological behavior of polymer blends and not valid for the entire testing frequency range.

3. Experimental Section

3.1. Materials. Two polyamide 6 (PA6) samples were used: a commercial one supplied by Heilongjiang Nylon Plastic Factory and a synthesized one in this lab. The number-average molar mass of the commercial one is 2.4×10^4 g/mol. And it is 7.1×10^3 g/mol for the synthesized one (measured by terminal amino group titration). An isotactic polypropylene used in this work was supplied by Beijing Yanshan Petrochemical Co. Ltd. Its mass average and number-average molar masses were $\bar{M}_w$

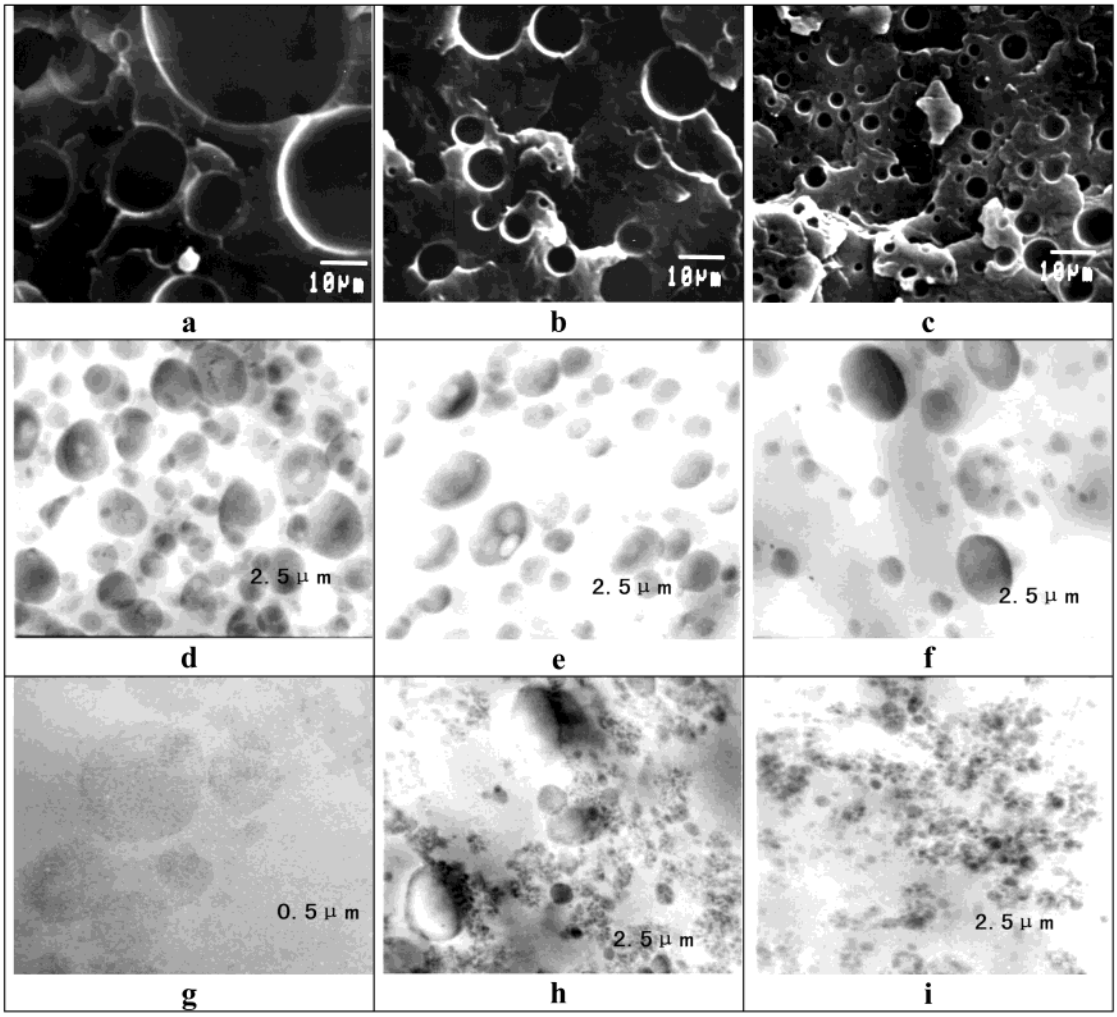

Figure 1. Micrographs of PP/PP-*g*-MAH/PA6 blends: (a) 90/ 0/10, (b) 80/0/20, (c) 70/0/30, (d) 45/45/10, (e) 40/40/20, (f) 35/35/30, (g) 45/45/10, (h) 40/40/20, and (i) 35/35/30. PA6C was adopted in parts a−f and PA6L was adopted in parts g−i.

$= 25.9 \times 10^4$and $\bar{M}_n = 6.5 \times 10^4$, respectively. A maleic anhydride polypropylene (PP-*g*-MAH) was supplied by Elf Atochem (trade name: CA100). Its mass average and number-average molar masses were $M_w = 5.93 \times 10^4$ $M_n = 3.2 \times 10^4$, respectively. The maleic anhydride content in the polymer was 1.03 wt %.

3.2. Preparation of PP/PP-*g*-MAH/PA6 Blends. PP/PP-*g*-MAH/PA6 blends were prepared by using an internal mixing chamber (Brabender Plasticord PLE 330). Prior to blending, PP, PP-*g*-MAH, and PA6 were dried in a vacuum oven at 70 °C for about 24 h. The mixing temperature was 230 °C. The rotating speed of the rotors was 50 revolutions per minute. The mixing time was 7 min. The dispersed phase of those blends was always PA6, and their matrixes were PP composed of PP + PP-*g*-MAH.

3.3 Rheological Measurement. The rheological behavior of PP/PA6 and PP/PP-*g*-MAH/PA6 blends were investigated by using a Physica-200 rheometer. A 25 mm parallel plate arrangement was adopted. The measuring temperature was 230 °C. Testing specimens were prepared by molding in a hot press at 230 °C and 5 MPa. Prior to compression molding, pellets were dried in a vacuum oven overnight. The rheometer chamber was purged with dry nitrogen during measurement to avoid degradation. A frequency range of 0.1−100 rad/s and a strain of 5% were supplied during the measurement. A strain sweep was carried out to determine the strain limit for linear viscoelastic responses.

3.4. Morphology Analysis. Morphology of samples of the ternary blending system was examined by using a JEOL JXA-840 scanning electron microscope (SEM) and a JEOL-2010 transmission electron microscope (TEM), respectively. For binary blending system, the morphology was only observed by SEM. To create better contrast, samples were fractured in liquid nitrogen, etched by formic acid to remove the PA6 particles. They were then coated with 50/50 Au/Pt to avoid charging. For compatibilized blending system, the TEM elastic bright-field images were taken. The accelerating voltage was 200 000 V. Ultrathin films of about 60 nm in thickness were obtained from quenched disks using a Leica Ultracut-E microtome with a diamond knife. They were treated with RuO_4 vapor in order to increase contrast.[32,33] As the staining rate of the PP phase was slower than that of the PA6, the PA6 domains were darker than that of the PP in the blends. The radius of the particles was determined from several representative photographs.

4. Results and Discussion

4.1. Morphology. The micrographs of a series of PP/PP-*g*-MAH/PA6 blends are shown in Figure 1. In the compatibilized blending systems, the amounts of PP and PP-*g*-MAH were always equal. PA6C represents the commercial PA6 and PA6L, the laboratory made one. The radii of the PA6 domains were on the order of 10 μm for the uncompatibilized blends and were in the submicrometer range for the compatibilized ones (see Table 1). It appears that the particle size distribution of the uncompatibilized blends, characterized by the ratio between the volume and number-average radii, R_v/R_n, was higher than the related values of compatibilized counterparts.

Table 1. Average Particle and Distributions for PP/PP-*g*-MAH/PA6 Blend

PP/PP-*g*-MAH/PA6 blend	φ_{PA6}[a]	R_v (μm)	R_n (μm)	R_v/R_n
90/0/10 (C)	0.081	5.7	3.59	1.59
80/0/20 (C)	0.156	18.3	8.5	2.15
70/0/30 (C)	0.254	35.4	13.0	2.7
45/45/10 (C)	0.081	0.22	0.16	1.34
40/40/20 (C)	0.156	0.33	0.18	1.8
35/35/30 (C)	0.254	0.38	0.25	1.54
45/45/10 (L)	0.081	0.09	0.06	1.44
40/40/20 (L)	0.156	0.1	0.06	1.38
35/35/30 (L)	0.254	0.12	0.07	1.71

[a] The volume fractions of PA6 in the blends were calculated based on the following mass densities: $\rho_{PP} = 0.902$ g/cm^3 and $\rho_{PA6} = 1.14$ g/cm^3.

Table 2. Zero Shear Viscosities of Blending Components

polymer component	η_0 at 230 °C (?), Pa.s
PP	3000
PP/PP-*g*-MAH (50/50)	950
PA6C	1260
PA6L	113

4.2. Rheology. The zero shear viscosities of various components is shown in Table 2, and the dynamic storage modulus of different blends as a function of angular frequency are shown in Figures 2 and 3. The modulus of a blend corresponding to the second plateau at low frequencies increased with increasing weight fraction of PA6 therein (φ_i) and with decreasing viscosity ratio K between the PA6 and the PP phase. These results are in qualitative agreement with those reported in the literature.[22]

It should be pointed out that the mixtures of PP and PP-*g*-MAH in those blends were considered as one unique phase. That consideration was based on a work reported in the literature.[34] (see Supporting Information I for detailed analysis).

4.3 Interfacial Tension. The interfacial tension between PP and PA6 was calculated upon fitting the above experimental data to the Palierne model. The simplified version of Palierne model (eq 10 in the paper of Graebling et al.[22]) was not applicable for the systems studied in this work for at least two reasons. First of all, none of the two polymer components involved in the blends could be described by a single Maxwell model. Second, according to the literature,[35] it is unlikely that the systems obeyed the time−temperature-superposition principles (TTS) which would otherwise allow us to determine λ_D of eq 12 in the paper of Graebling et al.[22] Thus eq 2 of this paper was used to do the job.

In the case of the uncompatibilized PP/PA6 blends, it was assumed that mechanical interactions between the two phases were weak to the point that $\beta_1^* = \beta_2^* = 0$. Very good agreement was obtained between the experimental data and the simulated ones for the PP/PA6C = 90/10 blend (Figure 4a). The interfacial tension used was 9.2 mN/m, which is very close to the one reported in the literature.[30] However, the agreement was not very good for the PP/PA6C = 70/30 blend when the same interfacial tension was used (Figure 4b). These features can be tentatively explained as follows: the particle size distribution in the PP /PA6C = 70/30 blend is relatively wide ($R_v/R_n = 2.7$). According to the literature,[22] eq 2 can be applicable only when the disperse particle size distribution is narrow enough ($R_v/R_n < 2$). To confirm the above argument, these two blending samples were presheared under low frequencies (0.1 s^{-1}) for 10 min prior to oscillatory experiments. Preshearing at low frequencies would favor coalescence of the PA6 domains therein, which would make them more uniform while average size would not change so much.[36] As shown in Figure 5, after preshearing the dynamic storage modulus of the blend of PP/PA6C = 90/10 did not change. But, obvious modification of the dynamic storage modulus happened for the blend of PP/PA6C = 70/30. More obvious shift could be observed in the low-frequency region. The simulated and experimental data were in good agreement after preshearing. The value of the interfacial tension used for the simulation was 9.2 mN/m for both blends. Therefore, it can be concluded that eq 2 describes well the rheological property of the

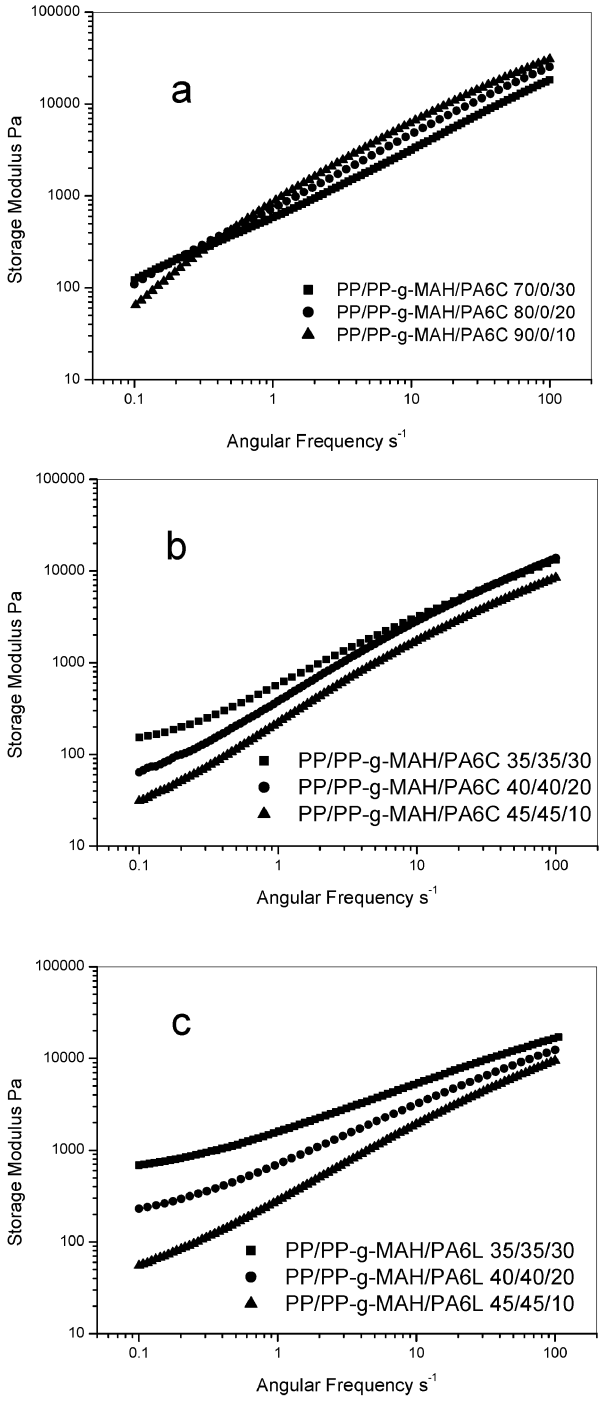

Figure 2. Dynamic storage modulus of PP/PP-*g*-MAH/PA6 blends as a function of angular frequency.

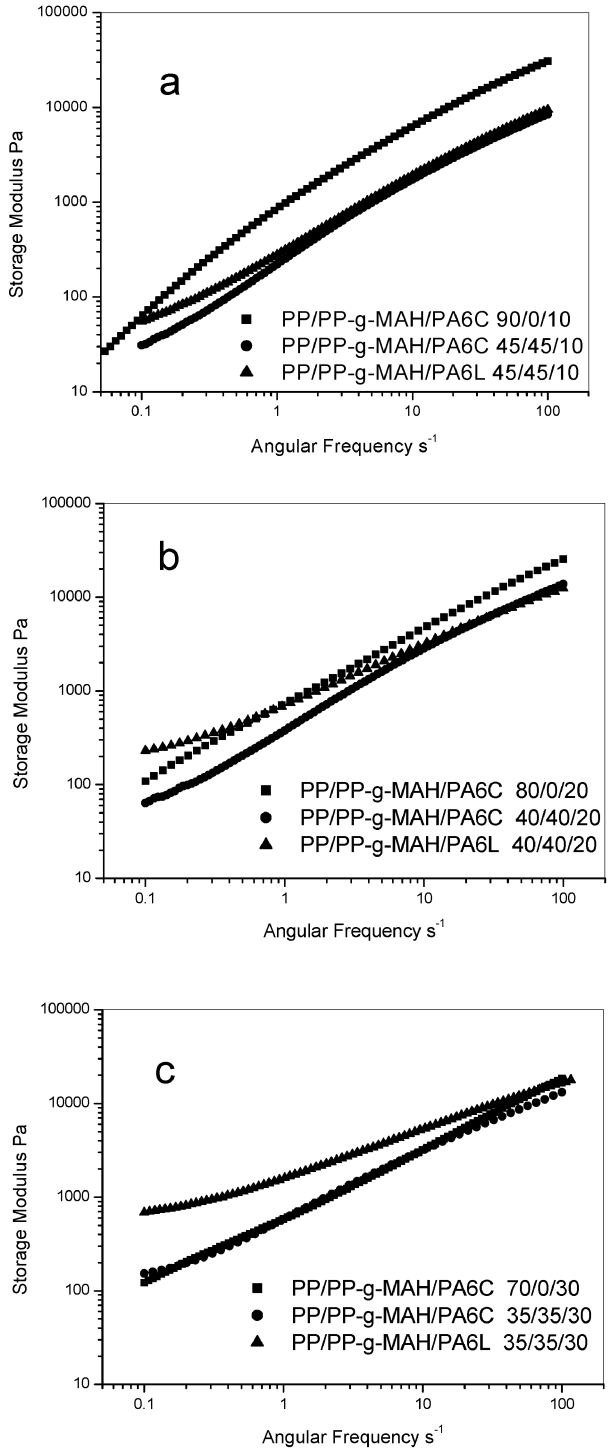

Figure 3. Dynamic storage modulus of PP/PP-*g*-MAH/PA6 blends as a function of angular frequency: (a) 10 wt % PA6; (b) 20 wt % PA6; (c) 30 wt % PA6.

uncompatibilized blends provided that the particle size distribution is small enough.

For ternary blends of PP/PP-*g*-MAH/PA6 the interfacial reaction between PP-*g*-MAH and PA6 had to be taken into account when eq 2 was used. It was assumed that the interfacial area did not change during the oscillatory test, thus $\beta_1^* = 0$. As for β_2^*, it was calculated based on the lightly cross-linked rubber model[37] (see Supporting Information II for details). The experimental and simulated dynamic storage moduli of PP/PP-*g*-MAH/PA6C (45/45/10) blend at different angular frequency are shown in Figure 6. The agreement was not

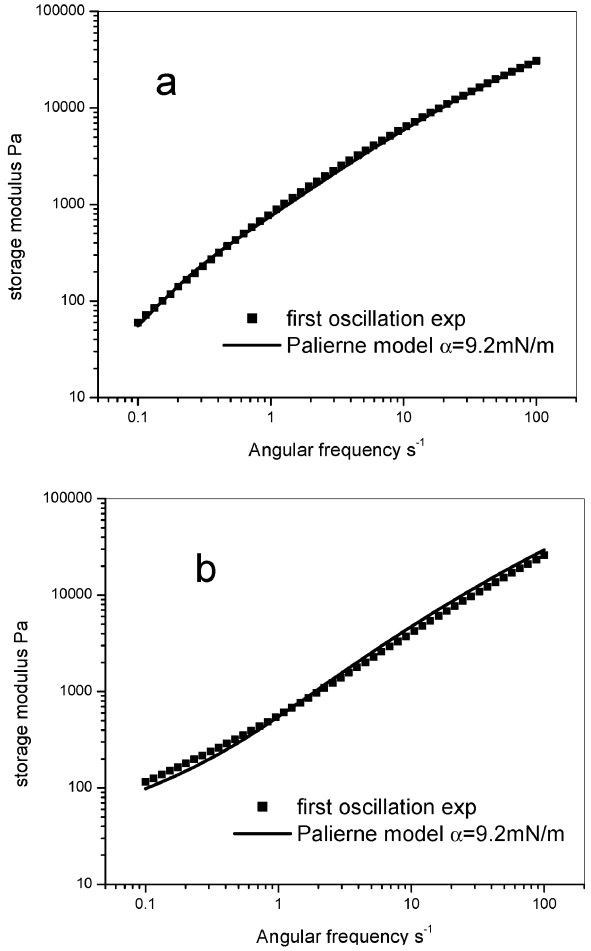

Figure 4. Dynamic storage modulus of PP/PA6C blends as a function of angular frequency: (a)PP/PA6C = 90/10; (b) PP/PA6C = 70/30.

good between the experimental and simulated data by using three different simulation scenarios: (1) both interfacial tension, α, and the plateau value of the storage modulus at low frequencies, β_0, were zero; (2) α = 1.6 mN/m and β_0 (α = 1.6 mN/m used here is just a choice. Better fitting could not be obtained with either higher or lower α value.); (3) α = 1.6 mN/m, $\beta_0 = 0.05$ and $\lambda_\beta = 0.08$ s (the last two parameters were obtained as explained in Supporting Information II). However, if preshear was adopted before rheological test a completely different situation was observed. Two preshear times, 10 and 20 min and one preshear frequency, 0.1 s^{-1} were used in this work. As shown in Figure 7, the value of the second plateau of the dynamic storage modulus tended to decrease with increasing preshear time. This seems to be that coalescence of PA6 particles took place in the ternary compatibilized blend, even the content of PA6 was low. Similar feature was not found in the binary uncompatibilized blend of PP/PA6 = 90/10 (seen in Figure 5).

The prediction of the dynamic storage modulus of a polymer blend by using eq 2 was built on the assumption that the morphology of domains in matrix was of emulsion type. As shown in Figure 1, PA6 particles in the binary blends were clearly of emulsion type and its dispersion in the PP matrix was very distinct. However, that was not exactly the case for the ternary blends, especially for those in which the laboratory-made PA6 was the dispersed phase. It seems to be that PA6 particles are more like emulsion-in-emulsion type.

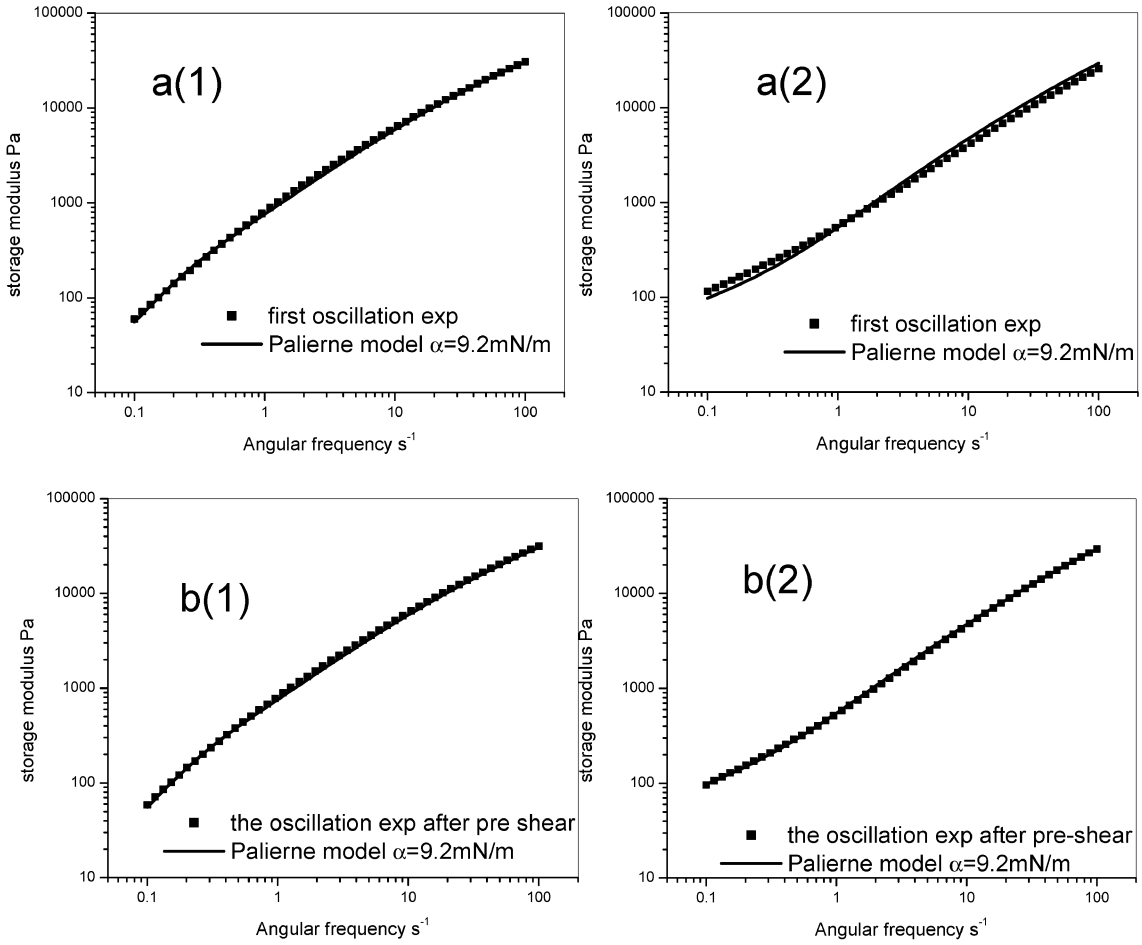

Figure 5. Dynamic storage modulus of PP/PA6C blends, shear rate = 0.1 $s^{-1}$and shear time = 10 min: (a1) PP/PA6C = 90/10 (without preshear); (a2) PP/PA6C = 70/30 (without preshear); (b1) PP/PA6C = 90/10 (with preshear); (b2) PP/PA6C = 70/30 (with preshear).

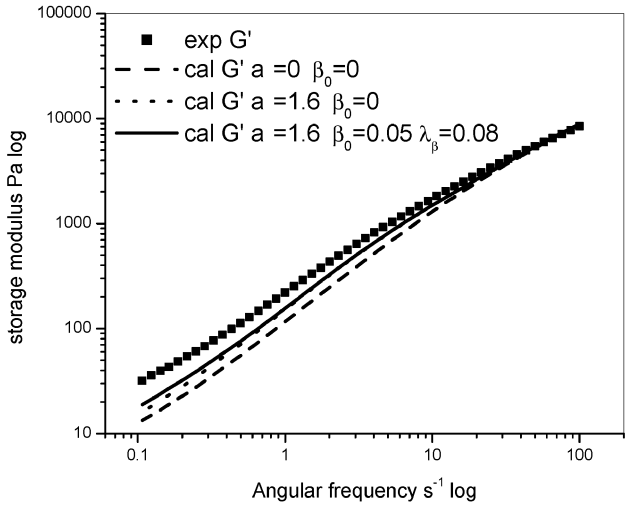

Figure 6. Comparison between simulated experimental dynamic storage modulus vs frequency curves for the PP/PP-*g*-MAH/PA6C (45/45/10) compatibilized blend without preshear.

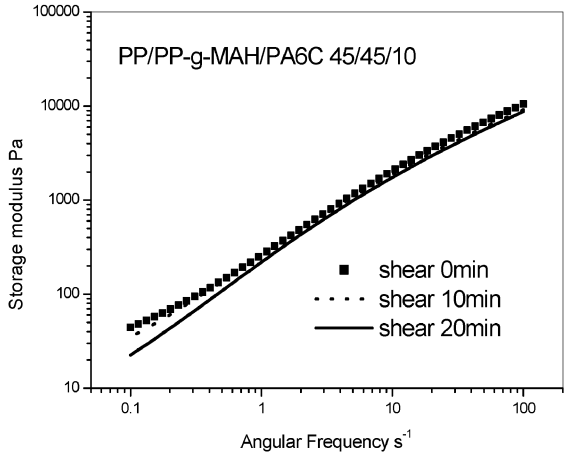

Figure 7. Effect of preshear time on the dynamic storage modulus of the ternary blends of PP/PP-*g*-MAH/PA6C = 45/45/10, shear rate = 0.1 s^{-1}. (The values on figure d to figure i represent the full width of each picture.)

Moreover, there exist both very small and very large particles. For the ternary blends based on the commercial PA6, the morphology of emulsion-in-emulsion type seems to be more visible when the PA6 content was high. The micrograph of a magnified PA6 particle of the ternary blend with PP/PP-*g*-MAH/PA6 = 35/35/30 is shown in Figure 8. This particle embedded in the PP + PP-*g*-MAH matrix. It seems to be composed of a PP and/or PP-*g*-MAH core and a PA6 and/or PP-*g*-PA6 shell. The thickness of the shell was not uniform. There were also many small particles located on the surface or in the vicinity of the shell. Those small particles might be micelles of PP-*g*-PA6 graft copolymer. In any event, the morphology of the ternary blends was much more complicated than a simple morphology of two-phase

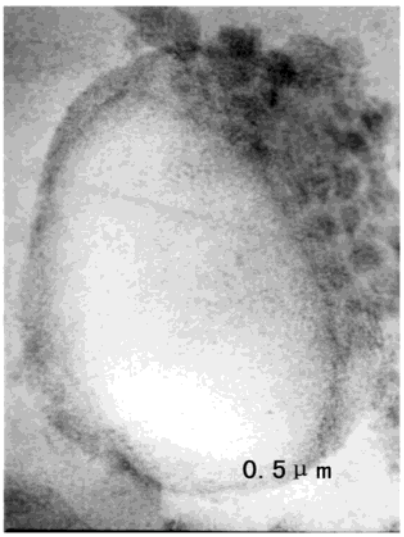

Figure 8. Micrograph of a magnified emulsion-in-emulsion type particle in the ternary blend of PP/PP-*g*-MAH/PA6 = 35/35/30. (The value 0.5 μm represents the full width of the picture.)

emulsion type. On this reason, it was not surprising that satisfactory results could not be obtained for predicting the dynamic storage modulus of a ternary blends as a function of angular frequency by using simply two-phase emulsion model.

As mentioned in the above paragraph, domains in the ternary blending system were consisting of core−shell particles with PP and/or PP-*g*-MAH as core and PA6 and/or PP-*g*-PA6 as shell. Following assumption was tentatively proposed in the simulation of dynamic modulus of a ternary blend by using eq 2. Here we took the total volume fraction of core−shell particles as the volume fraction of PA6 particles in the terminal zone. This consideration might be reasonable, since a particle as shown in Figure 8 with core−shell structure could be taken as independent unit to transfer shear stress. As the core−shell particles are much larger than those bare PA6 particles in the blend, so their form relaxation time should be much longer[27] and also they would have much larger contribution to the dynamic storage modulus in lower angular frequency zone than that with high frequency. In other words, the volume fraction of the PA6 phase used for simulation should be increased with the decrease of angular frequency and could be higher than the real value. Indeed, by using the increasing volume fraction to replace the pure constant PA6 volume fraction, better fitting was obtained for the simulated dynamic storage modulus curve as a function of angular frequency by using eq 2 with the experimental data in both the ternary blends of PP/PP-*g*-MAH/PA6C (45/45/10) and PP/PP-*g*-MAH/PA6L (45/45/10) treated by preshearing (shown in Figure 9). The interfacial tension value obtained by the simulation results is 2 mN/m for the PP/PP-*g*-MAH/PA6C blend and 1.5 mN/m for the PP/PP-*g*-MAH/PA6L blends, which were much smaller than the interfacial tension adopted in the simulation of PP/PA6 binary blending system. These results were in consistent with the literature.[30]

It was found that the interfacial modulus β_0 of the commercial PA6C was much lower than that of synthesized PA6L. This might be attributed to a higher content of PP-*g*-MAH-*g*-PA6L graft copolymer located in the interfaces between PP (or PP-*g*-MAH) and PA6L, since the synthesized PA6L had a much lower molar mass

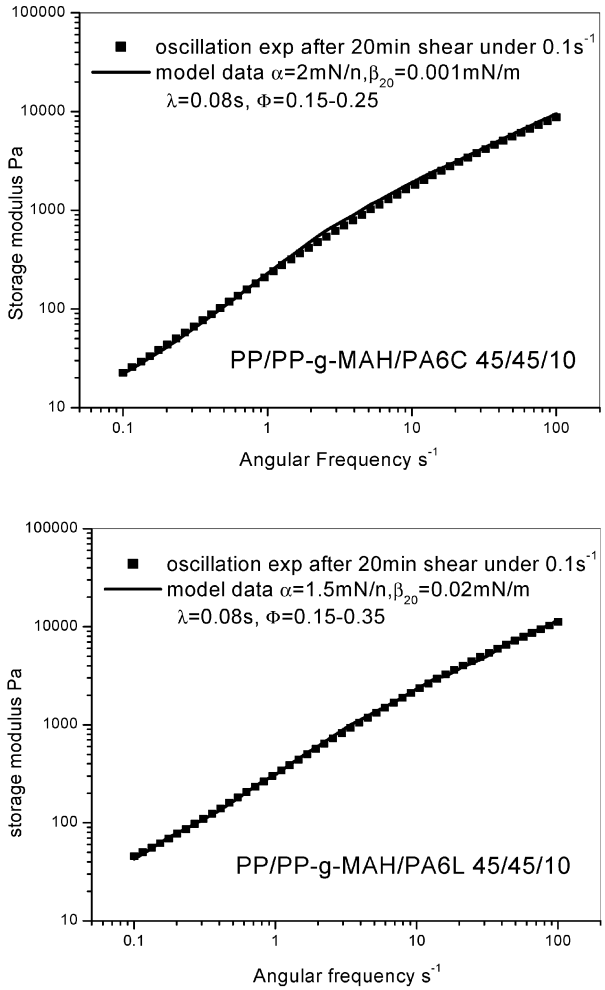

Figure 9. Dynamic storage modulus of PP/PP-*g*-MAH/PA6C (top) and PP/PP-*g*-MAH/PA6L (bottom) as a function of angular frequency.

and therefore more end-amino groups, which is in favor of the formation of PP-*g*-MAH-*g*-PA6L copolymer.[5,38,39]

5. Conclusion

In this work, the Palierne emulsion type model was used to describe the relationship between the rheological response to small amplitude oscillatory deformation and morphology of reactively compatibilized polymer blends. Blends based on polypropylene (PP), maleic anhydride grafted polypropylene (PP-*g*-MAH) and polyamide 6 (PA6) (PP + PP-*g*-MAH/PA6) blends were used for the study. The Palierne emulsion type model described very well the linear viscoelastic responses of uncompatibilized binary PP/PA6 blends and failed to do so for ternary compatibilized blends with PP-*g*-MAH. The latter was attributed to the fact that the morphology of the compatibilized blends was not of emulsion type with the PA6 particles dispersed in the PP matrix but of emulsion-in-emulsion type, i.e., PA6 particles dispersed in the PP matrix contained themselves PP or PP-*g*-MAH inclusions. Interestingly, if the PP-in-PA6 particles were considered as pure PA6 particles and if the volume fraction of the PA6 phase was increased accordingly, then the Palierne emulsion type model worked well. Preshear at low frequencies modified the morphology of both uncompatibilized and compatibilized blends. The particles of the dispersed phase (PA6) became more uniform. All those results showed that the Palierne

emulsion type model could be used to extract information on rheological properties and interfacial tension of polymer blends from known morphology and vice versa.

Acknowledgment. The authors would like to acknowledge the financial support of the Special Funds for Major State Basic Research Projects (G19990648) and the National Natural Science Foundation of China (59873022). Much appreciation was also given to Professor Guo-Hua Hu, Laboratoire des Sciences du Génie Chimique, Ecole Européenne d'Ingénieurs en Génie des Matériaux.

Supporting Information Available: Text giving (I) an analysis of the mixing of PP and PP-*g*-MAH and (II) the calculation of β_2^* based on the lightly cross-linked rubber model. This material is available free of charge via the Internet at http://pubs.acs.org.

References and Notes

(1) Paul, D. R.; Barlow, J. W.; Keskkula, H. In *Encyclopedia of Polymer Science and Engineering*, 2nd ed.; Kroschwitz, J. K., Ed.; Wiley: New York, 1998; Vol. 12.
(2) Baker, W.; Scott, C.; Hu. G. H. *Reactive Polymer Blending*; Hanser Publishers: Munich, Germany, 2001.
(3) Paul, D. R.; Newman, S. *Polymer Blends*; Academic: New York, 1976; Vols. 1 and 2.
(4) Xanthos, M. *Polym. Eng. Sci.* **1988**, *25*, 1392−1400.
(5) Utracki, L. A. *Two-Phase Polymer Blends*, Hanser: Munich, Germany, 1991.
(6) Garmabi, H.; Demarquette NR.; Karnal MR. *Int. Polym. Proc.* **1998**, *XIII*, 183−191.
(7) Wu, S. *Polymer Interface and Adhesion*; Marcel Dekker: New York, 1982.
(8) Ellingson, P. C.; Strard, D. A.; Cohen, A.; Sammler, R. L.; Carriere, C. J. *Macromolecules* **1994**, *27*, 1643−1647.
(9) Carriere, C. J.; Cohen, A.; Arends, C. B. *J. Rheol.* **1989**, *33*, 681.
(10) Carriere, C. J.; Cohen, A.; Arends, C. B. *J. Rheol.* **1991**, *35*, 205.
(11) Machiels, A. G. C.; Busser, R. J.; Van Dan, J.; de Boer, P. *Polym. Eng. Sci.* **1998**, *38*, 536−548.
(12) Scholz, P.; Froelich, D.; Muller, R. *J. Rheol.* **1989**, *33*, 481−499.
(13) Graebling, D.; Froelich, D.; Muller, R. *J. Rheol.* **1989**, *33*, 1283−1291.
(14) Graebling, D.; Muller, R. *Colloid Surf.* **1991**, *55*, 89−103.
(15) Graebling, D.; Benkira, A.; Gallot, Y.; Muller, R. *Eur. Polym. J.* **1994**, *30*, 301−308.
(16) Gramespacher, H.; Meissner, J. *J. Rheol.* **1992**, *36*, 1127−1141.
(17) Glennser, W.; Bruan, H.; Friedrich, C.; Cantow, J. *Polymer* **1994**, *35*, 128−135.
(18) Bousmina, M.; Bataille, P.; Sapieha, S.; Schreiber, H. P. *J. Rheol.* **1995**, *39*, 499−517.
(19) Lacroix, C.; Aressy, M.; Carreau, P. J. *Rheol. Acta*, **1997**, *36*, 416−428.
(20) Lacroix, C.; Girmela, M.; Carreau, P. J. *J. Rheol.* **1998**, *42*, 41−42.
(21) Brahimi, B.; Ait-Kadi, A.; Aiji, A.; Jéone, R.; Fayt, R. *J. Rheol.* **1991**, *35*, 1069−1091.
(22) Graebling, D.; Muller, R.; Palierne, J. P. *Macromolecules* **1993**, *26*, 320−329.
(23) Palierne, J. F. *Rheol. Acta* **1990**, *29*, 204−214.
(24) Germain, Y.; Ernst, B.; Genelot, O.; Dhamani, L. *J. Rheol.* **1994**, *38*, 681−691.
(25) Choi, S. J.; Schowalter, W. R. *Phys. Fluids* **1975**, *18*, 420−427.
(26) Oldryod, J. G. *Proc. R. Soc.: London Ser.* **1953**, *A218*, 122−132.
(27) Remain, R. E.; Cantow, H. J.; Friedrich, C. *Macromolecules* **1997**, *30*, 5476−5484.
(28) Puyvelde, P. V.; Velankar, S.; Moldenaers, P. *Curr. Opin. Colloid Interface Sci.* **2001**, *6*, 457−463.
(29) O'Shaughnessy, B.; Sawhney, U. *Macromolecules* **1996**, *29*, 7230−7239.
(30) Asthana, H.; Jayaraman, K. *Macromolecules* **1999**, *32*, 3412−3419.
(31) Jacbos, U.; Fahriander, M.; Winterhalter, J.; Friedrich, C. *J. Rheol.* **1999**, *43*, 1495−1509.
(32) Trent, J. S.; Scheinbeim, J. I.; Couchman, P. R. *Macromolecules* **1983**, *16*, 589.
(33) Montezinos, D.; Wells, B. G.; Burns, J. L. *J. Polym. Sci., Polym. Chem. Ed.* **1985**, *23*, 421.
(34) Gonealez-Montiel, A.; Keskkula, H.; Paul, D. R. *J. Polym. Sci., Part B: Polym. Phys.* **1995**, *33*, 1751−1767.
(35) Van Gurp, M.; Palmen, J. *Rheol. Bull.* **1998**, *67*, 5−8.
(36) Vinckier, I.; Laun, H. M. *Rheol. Acta* **1999**, *38*, 274−286.
(37) Ferry, J. D. *Viscoelastic properties of Polymers*; John Wiley & Sons Inc.: New York and London, 1980.
(38) Hu, G. H.; Lambla, M, *J. Polym. Sci., Chem. Ed.* **1995**, *33*, 97−107.
(39) Hu, G. H.; Kadri, I, *J. Polym. Sci., Part B: Phys. Ed.* **1998**, *36*, 2153.
(40) Flory, P. J. *Principles of Polymer Chemistry*; Cornell University Press: Ithaca, NY, 1953.
(41) Koningsweld, R.; Schoffaleers, H. M. *Pure Appl. Chem.* **1974**, *39*, 1.
(42) Ten-Brinke, G.; Karase, F. E.; Masknight, W. J. *Macromolecules* **1983**, *16*, 1827.

MA020595D